Fundamentals of Radiation Oncology for Treatment of Vertebral Metastases

Sujana Gottumukkala, MD, MPH
Udayan Srivastava, MD
Samantha Brocklehurst, BS
J. Travis Mendel, MD
Kiran Kumar, MD
Fang F. Yu, MD
Amit Agarwal, MD
Bhavya R. Shah, MD
Shaleen Vira, MD
Karuna M. Raj, MD

The fields of both radiology and radiation oncology have evolved considerably in the past few decades, resulting in an increased ability to delineate between tumor and normal tissue to precisely target and treat vertebral metastases with radiation therapy. These scientific advances have also led to improvements in assessing treatment response and diagnosing toxic effects related to radiation treatment. However, despite technological innovations yielding greatly improved rates of palliative relief and local control of osseous spinal metastases, radiation therapy can still lead to a number of acute and delayed posttreatment complications. Treatment-related adverse effects may include pain flare, esophageal toxic effects, dermatitis, vertebral compression fracture, radiation myelopathy, and myositis, among others. The authors provide an overview of the multidisciplinary approach to the treatment of spinal metastases, indications for surgical management versus radiation therapy, various radiation technologies and techniques (along with their applications for spinal metastases), and current principles of treatment planning for conventional and stereotactic radiation treatment. Different radiologic criteria for assessment of treatment response, recent advances in radiologic imaging, and both common and rare complications related to spinal irradiation are also discussed, along with the imaging characteristics of various adverse effects. Familiarity with these topics will not only assist the diagnostic radiologist in assessing treatment response and diagnosing treatment-related complications but will also allow more effective collaboration between diagnostic radiologists and radiation oncologists to guide management decisions and ensure high-quality patient care.

Abbreviations: CEBRT = conventional external-beam radiation therapy, CRT = conformal radiation therapy, CTV = clinical target volume, ESCC = epidural spinal cord compression, GTV = gross tumor volume, IMRT = intensity-modulated radiation therapy, OAR = organ at risk, PTV = planning target volume, SABR = stereotactic ablative radiation therapy, SBRT = stereotactic body radiation therapy, 3D = three dimensional, VCF = vertebral compression fracture

RadioGraphics 2021; 41:2136–2156

https://doi.org/10.1148/rg.2021210052

Content Codes: NR RO

From the Department of Radiation Oncology (S.G., S.B., K.K.), Department of Radiology (U.S., F.F.Y., A.A., B.R.S., K.M.R.), and Departments of Orthopaedic Surgery and Neurosurgery (S.V.), The University of Texas Southwestern Medical Center, 5323 Harry Hines Blvd, Dallas, TX 75390; and Rio Grande Urology, El Paso, Tex (J.T.M.). Presented as an education exhibit at the 2020 RSNA Annual Meeting. Received March 22, 2021; revision requested April 30 and received May 27; accepted May 29. For this journal-based SA-CME activity, the authors F.F.U. and A.A. have provide disclosures (see end of article); all other authors, the editor, and the reviewers have disclosed no relevant relationships. **Address correspondence to** K.M.R. (e-mail: *karuna.raj@utsouthwestern.edu*).

SA-CME LEARNING OBJECTIVES

After completing this journal-based SA-CME activity, participants will be able to:

- Discuss the foundations of radiation treatment planning with regard to osseous metastatic disease involving the spine.
- Identify key imaging findings that help the radiation oncologist in accurate staging, treatment planning, and response assessment and surveillance after radiation therapy.
- Describe expected and unexpected posttreatment effects of radiation therapy.

See www.rsna.org/education/search/RG.

Introduction

The discovery of x-rays by William Roentgen in 1895 paved the way not only for the development of diagnostic radiology as a specialty but also for radiation oncology. The first treatment of cancer with radiation therapy occurred soon afterward in 1896. Radiation oncology has since evolved considerably, with radiation therapy playing a vital role in cancer treatment, along with surgery and systemic therapies. As therapeutic options have advanced, there

TEACHING POINTS

- Radioresistant tumors may undergo stereotactic radiation in cases of low-grade ESCC, but surgical separation is recommended for radioresistant tumors demonstrating high-grade ESCC.
- Mechanical stability is typically assessed with the Spinal Instability Neoplastic Score, an 18-point scale that categorizes on the basis of location of involved vertebra, functional pain, quality of bone lesion, radiographic spinal alignment, degree of vertebral body collapse, and posterior element involvement.
- Common target volumes contoured for treatment of the spine include GTV, CTV, and PTV.
- Treatment of radioresistant tumors with a smaller number of fractions with a higher radiation dose per fraction, such as in SABR, is more biologically effective than the same total dose given by using a larger number of fractions with a lower dose per fraction.
- Familiarity with radiation treatment planning and posttreatment complications associated with spinal irradiation is also crucial for radiologists in the interpretation of posttreatment images and detection of treatment-related toxic effects.

has been an increased emphasis on the management of both primary neoplasms and metastatic disease. Spinal malignancies are of particular interest, as their proximity to the spinal cord can result in a profound impact on quality of life. Although primary spinal tumors are rare, spine metastases are a common sequela for patients with metastatic cancer and account for the majority of newly diagnosed spine tumors (1). More than 180 000 spinal metastases are diagnosed each year and are the most common reason for spinal irradiation (2). If untreated, vertebral metastases can lead to pain, fracture, and loss of neurologic function.

Approach to Spinal Tumor Treatment

Given the advances in pharmacologic, surgical, and radiation treatment of spinal osseous metastatic disease, several factors must be considered to determine optimal therapeutic strategies. These include the presence of myelopathy or functional radiculopathy, radiosensitivity of the tumor based on histologic analysis results, spinal stability, comorbidities, and extent of disease. The NOMS decision framework developed by the Memorial Sloan-Kettering Cancer Center incorporates *n*eurologic, *o*ncologic, *m*echanical, and *s*ystemic considerations, providing a paradigm to guide treatment of spinal metastases and allowing multidisciplinary teams to use a common language to help develop individualized treatment plans (3) (Fig 1).

The neurologic portion of the framework includes assessment of the degree of spinal cord compromise, which includes a radiographic evaluation of the degree of epidural spinal cord compression (ESCC) and a clinical assessment of neurologic deficits. The likelihood of exhibiting myelopathy and/or functional radiculopathy is attributed to epidural tumor extension. Thus, assessment of the degree of ESCC is a critical factor in treatment decisions (3). A consensus ESCC scale developed by Bilsky et al (4) provides a tool that can be used to describe the degree of epidural disease based on T2-weighted MRI findings at the most severely involved level, and thus can help better inform treatment decisions (Fig 2).

The oncologic assessment takes into consideration the predicted responsiveness of tumor based on histology and history of prior irradiation. Radiosensitive tumors may be treated with radiation regardless of the degree of ESCC, avoiding the need for surgery. Several studies have confirmed that patients with favorable tumor histologies are more likely to demonstrate improvement in neurologic function and pain scores following radiation therapy. Radioresistant tumors may undergo stereotactic radiation therapy in cases of low-grade ESCC, but surgical separation is recommended for radioresistant tumors demonstrating high-grade ESCC. In separation surgery, the tumor margin is resected from the spinal cord, allowing postoperative tumor control with stereotactic body radiation therapy (SBRT) and avoiding toxic effects to the spinal cord (at least 2 mm of separation between the cord and tumor is required for optimal delivery of cytotoxic doses of radiation to the tumor). This approach, in turn, leads to a decrease in morbidity associated with aggressive surgical resection such as corpectomy (3). Separation surgery has become increasingly common as adjuvant radiation therapy options have evolved, but complete tumor resection is still preferred in patients with good performance status and life expectancy. Regardless of whether corpectomy or separation surgery is chosen, surgical resection frequently requires adjuvant radiation therapy to sterilize the surgical field and account for microscopic disease.

In patients with metastases causing high-grade ESCC, decompression and stabilization followed by adjuvant radiation therapy is recommended, owing to data demonstrating superior outcomes in terms of ambulation, bowel and bladder continence, and narcotic requirements compared with those of conventional radiation therapy alone (5). Thus, from a neurologic and oncologic perspective, patients with high-grade ESCC and radioresistant tumors are recommended to undergo surgical intervention before radiation therapy (3).

The mechanical portion of the assessment evaluates spinal instability on the basis of clinical and radiographic criteria. Clinically, patients with

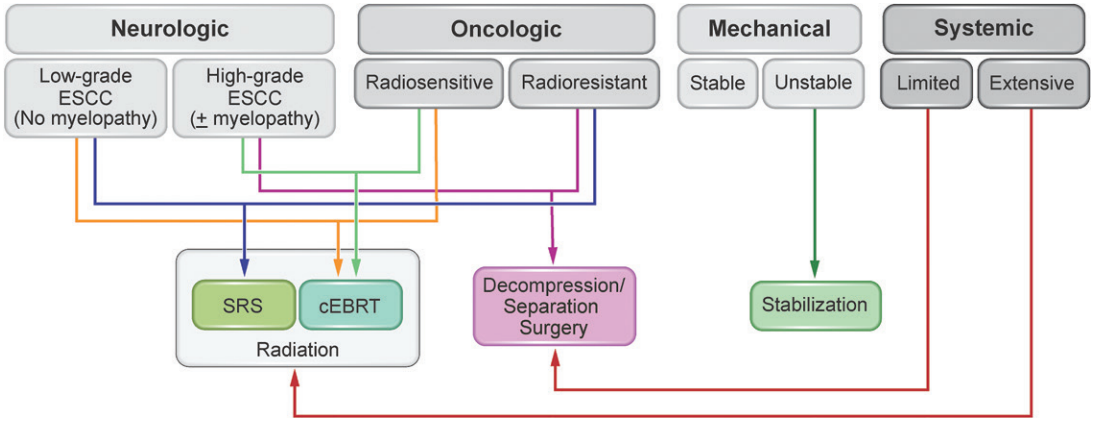

Figure 1. The NOMS framework provides a multidisciplinary paradigm that can be used to determine the optimal treatment of spinal metastases. *cEBRT* = conventional fractionated external-beam radiation therapy, *ESCC* = epidural spinal cord compression, *SRS* = stereotactic radiosurgery. (Adapted and reprinted, with permission, from reference 3.)

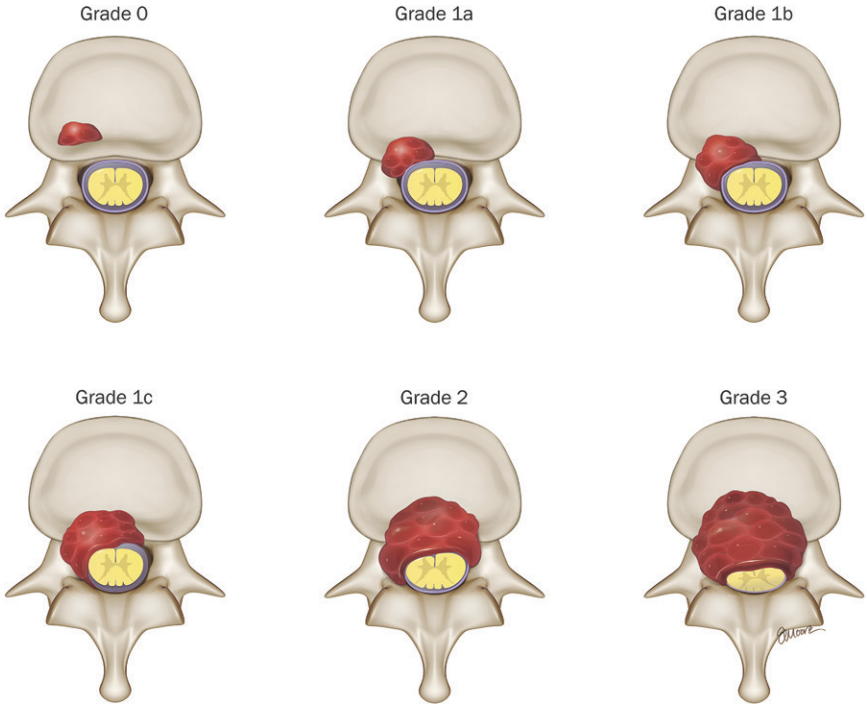

Figure 2. Schematic representation of the six-point Bilsky classification for epidural disease. According to the Bilsky scale, Grade 0 indicates bone involvement only. Grade 1a indicates epidural impingement without thecal sac deformation. Grade 1b indicates deformation of the thecal sac without abutment of the spinal cord. Grade 1c indicates deformation of the thecal sac with abutment of the spinal cord. Grade 2 describes spinal cord compression but with cerebrospinal fluid (CSF) visible around the cord. Grade 3 describes spinal cord compression without visible CSF. Bilsky grades 0 and 1 are considered low-grade ESCC, which is amenable to stereotactic radiation therapy. The subclassification of grade 1 is an important consideration in the safe delivery of cytotoxic doses of radiation to the tumor. For example, for grades 1a or 1b, the tumor can be treated while maintaining a 1–2 mm distance from the spinal cord, whereas high radiation doses to the tumor margins in the case of a grade 1c tumor could potentially result in an overdose to the spinal cord. However, newer radiation therapy techniques allow administration of adequate radiation doses needed for tumor control while avoiding spinal cord toxic effects. Separation surgery or conventional external-beam radiation therapy (CEBRT) is recommended for grades 2 and 3, which are classified as high-grade ESCC.

spinal instability present with severe movement-related pain (unrelieved with steroid therapy), symptomatic or progressive spine deformity, and/or neurologic compromise under physiologic loads. Regardless of the degree of ESCC and radiosensitivity of the tumor, mechanical instability is an independent indication for surgical stabilization or percutaneous vertebral augmentation (3,6).

Mechanical stability is typically assessed with the Spinal Instability Neoplastic Score, an 18-point scale that categorizes on the basis of location of involved vertebra, functional pain, quality of bone lesion, radiographic spinal alignment, degree of vertebral body collapse, and posterior element involvement (Table 1). A score of 7–12 signifies potential instability, while a score of 13–18 signifies definite instability; patients with a score greater than 7 should be referred for surgical stabilization (7).

In clinical practice, many patients score in the indeterminate category (score of 7–12), and the ultimate decision as to whether surgical decompression and stabilization is offered is based on

Table 1: Spine Instability Neoplastic Score

Characteristic	Score
Location	
Junctional (C0-C2, C7-T2, T11-L1, L5-S1)	3
Mobile spine (C3-C6, L2-L4)	2
Semirigid (T3-T10)	1
Rigid (S2-S5)	0
Pain relief with recumbency and/or pain with movement or spinal loading	
Yes	3
No (occasional pain but not mechanical)	1
Pain-free lesion	0
Bone lesion	
Osteolytic	2
Mixed (osteolytic and osteoblastic)	1
Blastic	0
Radiographic spinal alignment	
Subluxation or translation present	4
De novo deformity (kyphosis and/or scoliosis)	2
Normal alignment	0
Vertebral body collapse	
>50% collapse	3
<50% collapse	2
No collapse with >50% vertebral body involved	1
None of the above	0
Posterolateral involvement of the spinal elements	
Bilateral	3
Unilateral	1
None of the above	0

Source.—Adapted and reprinted, with permission, from reference 6.

patient factors not captured in the grading scale such as frailty, comorbidities, and the patient's expectations and/or goals of care. Indeed, clinical judgment could drive starkly different treatment plans for the identical radiologic appearance of a metastasis in two different patients with identical oncologic profiles. Nevertheless, the Spinal Instability Neoplastic Score framework allows the surgeon a platform to engage in shared patient-physician decision making and provides a common language for discussion among providers on the multidisciplinary oncologic team.

Assessment of systemic disease includes evaluation of the overall extent of disease and potential associated medical comorbidities to address the patient's ability to tolerate treatment, as well as overall survival. A thorough evaluation by the oncologist (with regard to metastatic staging and tumor histology) and surgical risk stratification are used to develop treatment plans. As discussed previously, common surgical treatment indications for spinal tumors include high-grade ESCC, neurologic deficits, mechanical instability, intractable pain, radioresistant histology, and post–radiation therapy tumor progression (3).

Radiation Treatment of Spinal Tumors

Radiation treatment of spinal tumors is delivered with external-beam radiation therapy for indications such as palliation of pain, preservation or recovery of neurologic function, or durable local tumor control in the oligometastatic setting. External-beam radiation therapy may be delivered as conventional fractionation, known as conventional external-beam radiation therapy (CEBRT), or with a stereotactic approach, known as stereotactic ablative radiation therapy (SABR) or stereotactic body radiation therapy (SBRT) (Fig 3). CEBRT consists of nonablative doses of radiation delivered in 1–15 treatments, known as fractions, which are typically delivered daily. CEBRT is often used for palliation in patients with poor performance status or for inoperable high-grade ESCC. In contrast, SABR is an ablative treatment consisting of fewer fractions, usually 1–5, with higher doses of radiation per fraction. Treatment is generally delivered with an interval of a few days between fractions. SABR is typically recommended for de novo metastases, postoperative radiation, or reirradiation. When used in a de novo or postoperative setting, SABR has been shown to achieve pain response and local control rates of 80%–95% (8–10). Patients receiving adjuvant radiosurgery in the setting of reirradiation have demonstrated similar rates of local control and pain relief compared with those with no history of prior radiation (11).

Radiation Treatment Planning and Types of Radiation Therapy

The fundamental rationale for radiation therapy in cancer treatment is to preferentially damage malignant cells while avoiding or limiting damage to normal tissues. To achieve this goal, patients undergo rigorous treatment planning, beginning with CT simulation. During CT simulation, various immobilization devices are used to position patients in a way that can be reproduced during treatment with minimal interfraction and intrafractional variability. A CT image is then obtained for the purpose of radiation planning, which involves delineation of the target and normal tissues, also known as organs at risk (OARs), in a process referred to as contouring. CT also allows algorithmic calculation of radiation dose

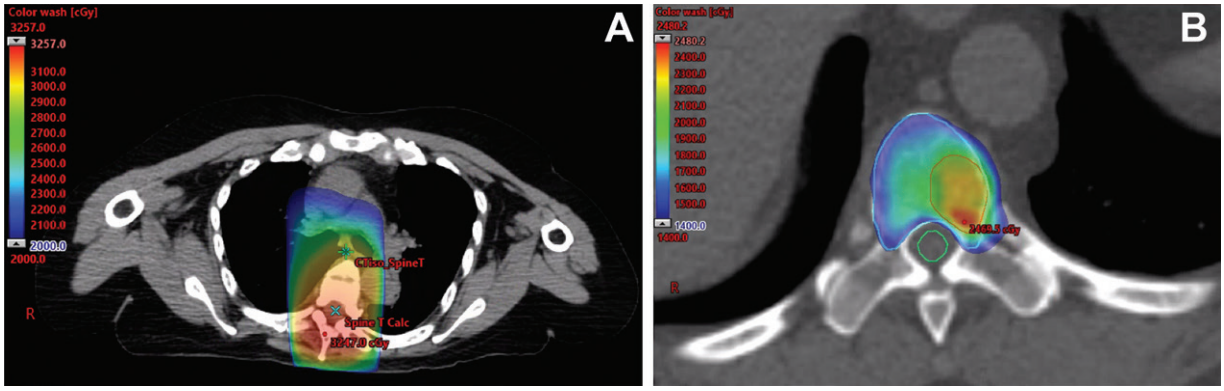

Figure 3. Spinal metastases treated with radiation therapy. **(A)** Axial dosimetric CT image shows CEBRT with 30 Gy in 10 fractions. **(B)** Axial dosimetric CT image shows SABR with 14 Gy to the vertebral body (cyan outline) and 20 Gy to the gross tumor (red outline) delivered in a single fraction. Compared with CEBRT, SABR is more technically challenging in terms of setup, planning, and treatment delivery but results in more conformal dose distribution and sharper dose fall off, resulting in increased sparing of normal tissues.

deposition. Additional imaging modalities such as MRI and PET may be fused to CT images to improve tumor visualization.

Contouring involves delineating several target volumes, as well as any OARs with close proximity to the tumor. Common target volumes contoured for treatment of the spine include gross tumor volume (GTV), clinical target volume (CTV), and planning target volume (PTV). The GTV is contoured as visible tumor that is appreciable at radiographic or clinical examination. The GTV is then expanded to generate a CTV, which accounts for possible areas of microscopic tumor infiltration. The CTV is further expanded to create a PTV, which accounts for interfraction variability due to patient motion and setup uncertainty. It should be noted that GTV is not always contoured in palliative cases involving the complete treatment of multiple adjacent vertebral bodies (Fig 4).

The radiation prescription includes treatment site, total radiation dose, total number of fractions, dose per fraction, treatment technique, beam energy, and frequency of treatment. When determining the fractionation regimen and choosing between use of CEBRT and SABR, consideration of tumor histology is vital. Radiosensitive histologies, such as those of breast cancer, prostate cancer, myeloma, lymphoma, seminoma, and leukemia, have demonstrated durable response to conventional fractionation (12). In contrast, radioresistant histologies such as non–small cell lung cancer, gastrointestinal cancer, melanoma, renal cell carcinoma, and sarcoma require more potent radiation doses for effective palliation and tumor control. Treatment of radioresistant tumors with a smaller number of fractions with a higher radiation dose per fraction, such as in SABR, is more biologically effective than the same total dose given by using a larger number of fractions with a lower dose per fraction. Studies have shown excellent outcomes including local control rates as high as 90% when treating radioresistant oligometastatic tumors with SABR (13,14). The choice of prescription dose, measured in units of gray (Gy), is dependent on a number of factors including tumor histology, treatment setting (de novo, adjuvant, reirradiation, etc), tumor proximity to OARs, and the decision to use CEBRT or SABR.

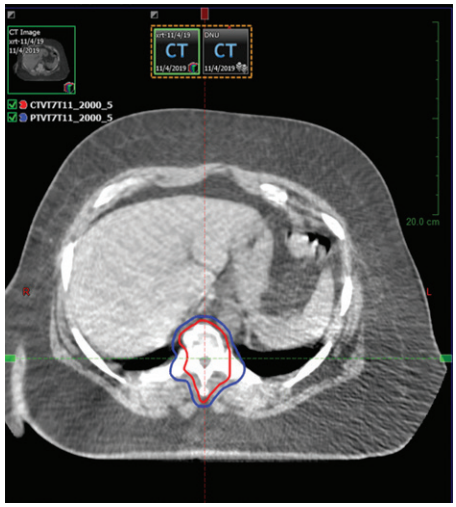

Figure 4. Palliative treatment with CEBRT for metastatic prostate cancer to the thoracic spine. Axial dosimetric CT image obtained for treatment planning shows that a total dose of 20 Gy in five fractions was delivered. The CTV is outlined in red, and the PTV is outlined in blue. In palliative CEBRT cases such as this example, it is not always considered necessary to contour the GTV.

Conventional External-Beam Radiation Therapy.—In CEBRT, CT simulation typically involves placing the patient in the supine position with immobilization by using a long Vac-Lok bag (MED-TEC), an inflatable device shaped

Table 2: Dose Constraints for Five-Fraction Irradiation of OARs

OAR	Irradiated Tissue Volume	Maximal Radiation Dose (Gy)	Maximal Radiation Point Dose (Gy)	End Point
Spinal cord	<0.35 cc	22	28	Myelitis
Cauda equina	<5 cc	30	31.5	Neuritis
Esophagus	<5 cc	32.5	38	Esophagitis
Lung	<1500 cc (men)	12.5	…	Basic lung function
	<950 cc (women)	12.5	…	Basic lung function
	<37%	13.5	…	Pneumonitis

Note.—The restricted doses listed are those used for five-fraction irradiation at the authors' institution (The University of Texas Southwestern Medical Center). The maximal point dose is measured as the maximal dose to 0.035 cc.

to the patient's body. A knee sponge is also used to provide support during positioning and to increase patient comfort. CEBRT requires the radiation oncologist to place an isocenter on the CT image obtained at simulation. The isocenter is the intersection for gantry, couch, and collimator revolution and is important for the calculation of radiation dose, as well as for treatment setup and delivery. Following designation of the isocenter during simulation, the patient is marked with small tattoos or stickers that are used during treatment setup to triangulate to the isocenter for each treatment.

Target delineation in CEBRT to the spine follows the same general principles as other disease sites, with GTV contoured as visible disease at imaging. CTV expansion typically includes the entire involved vertebral body with a further 5-mm to 1-cm expansion to generate the PTV. Given the relatively large target and spinal cord radiation dose constraints, CEBRT is limited to nonablative dose delivery to the spine.

There are a number of possible fractionation schemes in CEBRT including 8 Gy in one fraction, 20 Gy in five fractions, and 30 Gy in 10 fractions. These fractionation regimens all have similar effectiveness for pain relief, although the retreatment rate is higher in patients receiving 8 Gy in one fraction (15–17). Radiation dose constraints for OARs can vary considerably by institution. Tables 2 and 3 show the authors' institutional radiation dose constraints for five-fraction and 10-fraction treatment regimens, which are the most commonly used conventional fractionation schemes at our institution.

Stereotactic Ablative Radiation Therapy.—Compared with CEBRT, SABR is more technically challenging in terms of setup, planning, and treatment delivery. However, the increased conformality and sharper radiation dose fall-off allow increased sparing of normal tissues, permitting delivery of higher radiation doses per fraction than in CEBRT and allowing reirradiation (Fig 5). Simulation requirements differ significantly between SABR and CEBRT, beginning with section thickness. While a CT section thickness of 3–5 mm is acceptable for CEBRT, 1–2-mm sections are preferred for SABR. Furthermore, while SABR does not require placement of an isocenter during CT simulation, patients must be referenced to their immobilization devices, with the immobilization device in turn referenced to the treatment couch. Patients are positioned supine, and the immobilization device used varies depending on the location of the tumor. A body frame, headrest, long Vac-Lok bag, and knee sponge are typically used for immobilization of patients with tumors located in the lumbar and lower thoracic spine, and patients are typically positioned with their arms above their head. A leg laser is used for patient marking, and an arch is used to place sternal tattoos that reference the patient to the body frame. In contrast, patients with tumors in the cervical or upper thoracic spine are typically immobilized with a headrest, Aquaplast mask (Qfix), and S-frame. The S-frame is placed on the treatment couch, and the patient is positioned with their arms at their sides. The Aquaplast mask is shaped to the patient's head and shoulders and clipped into the S-frame, effectively immobilizing the patient's upper body. The Aquaplast mask is marked to ensure a reproducible setup for each treatment (Fig 6).

Target delineation in SABR typically follows the paradigm outlined in the International Spine Radiosurgery Consortium Consensus (ISRC) guidelines, with both the GTV and CTV treated to the same ablative dose (18). However, it is unclear if treating both the GTV and CTV with such high ablative doses of radiation is necessary for local control or if this approach increases toxic effects without providing benefit. To mitigate the possible risk of increased toxic effects with high doses to the CTV, the

Table 3: Dose Constraints for 10-Fraction Irradiation of OARs

OAR	Irradiated Tissue Volume	Maximal Radiation Dose (Gy)	Maximal Radiation Point Dose (Gy)	End Point
Spinal cord	<5 cc	31	36	Myelitis
Cauda equina	<5 cc	35	41	Neuritis
Esophagus	<5 cc	40	48	Esophagitis
Lung	<1500 cc (men)	15	…	Basic lung function
	<950 cc (women)	15	…	Basic lung function
	<37%	16	…	Pneumonitis

Note.—The restricted doses listed are those used for 10-fraction irradiation at the authors' institution (The University of Texas Southwestern Medical Center). The maximal point dose is measured as the maximal dose to 0.035 cc.

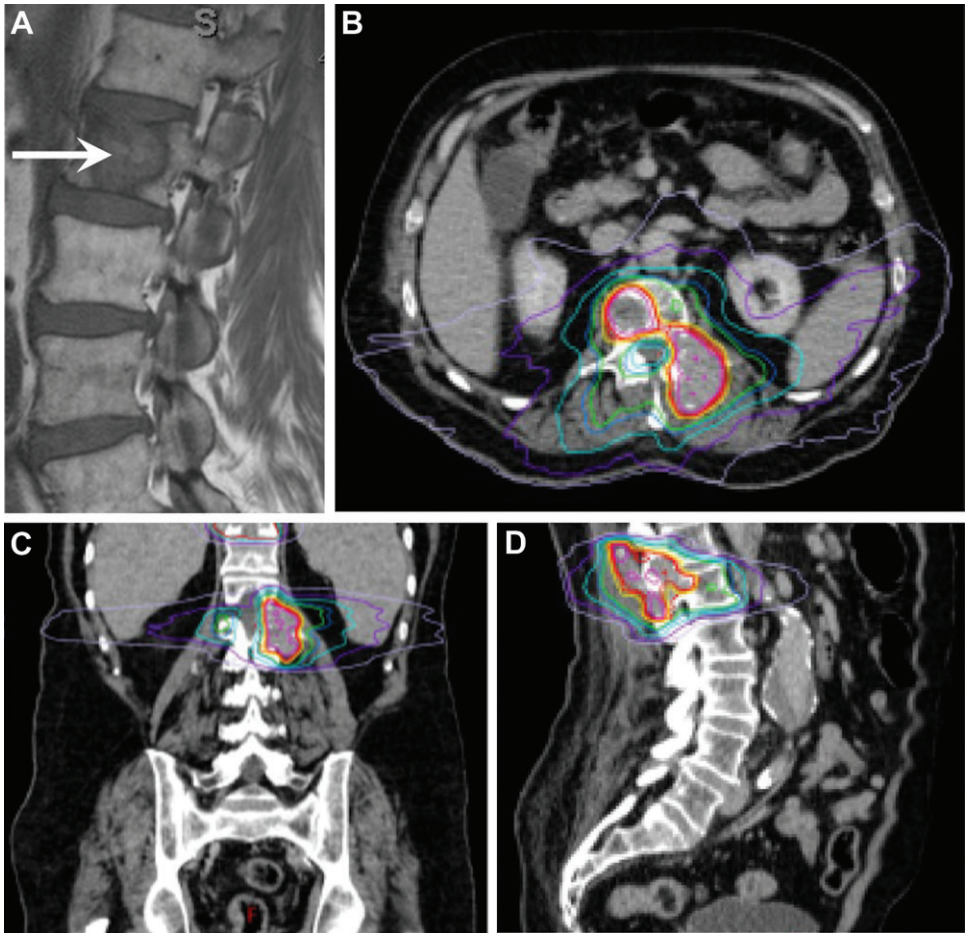

Figure 5. Treatment of metastatic Hurthle cell carcinoma with SABR. **(A)** Sagittal T1-weighted MR image shows an L2 metastasis (arrow). **(B–D)** Axial **(B)**, coronal **(C)**, and sagittal **(D)** dosimetric CT images were obtained for SABR treatment planning. SABR is frequently used for de novo metastases, adjuvant treatment following surgical resection, or for reirradiation to recurrent or progressive tumors. As this patient had previously received radiation to the lumbar spine, he underwent reirradiation therapy with SABR, with a total dose of 40 Gy in five fractions.

authors' institution uses a protocol in which a novel dose-painting simultaneous integrated boost (SIB) technique is used to treat the CTV, as defined by International Standard Recording Code (ISRC) guidelines, to a lower dose while simultaneously delivering a high ablative dose to the GTV (Fig 7). It is hypothesized that the lower radiation dose to the CTV is sufficient to control microscopic disease while also reducing radiation dose to adjacent OARs, decreasing the risk of toxic effects and allowing for future reirradiation if necessary (Fig 8).

Figure 6. Photographs show a CT simulation setup for SABR to the lumbar or lower thoracic spine **(A)** and cervical or upper thoracic spine **(B)**. **(A)** For treatment of the lumbar or lower thoracic spine, the patient is placed in a long Vak-Lok bag (red *A*) within the SBRT body frame (red *B*), with a knee sponge (red *C*) under the knees and with the patient's arms up. The leg laser (red *D*) and arch (red *E*) are used for patient marking. **(B)** For treatment of the cervical or upper thoracic spine, the patient is positioned with arms down and the S-frame (red *F*), with an Aquaplast mask (red *G*) used rather than the body frame.

Fractionation schemes can vary widely between institutions. Commonly used fractionation regimens include 16–24 Gy in one fraction, 20–24 Gy in two fractions, 24–40 Gy in three fractions, and 25–40 Gy in five fractions (10,19–21). Radiation dose constraints to the spinal cord vary depending on fractionation, but a maximum point dose of 14 Gy to the spinal cord is widely accepted for single-fraction treatment regimens (22). Tables 4 and 5 show our institutional radiation dose constraints for one-fraction and three-fraction treatment regimens, which are the most commonly used SABR fractionation schemes at our institution.

Tools and Techniques

As the field of radiation oncology has evolved, so too has the complexity of the treatment machines and techniques available for treatment planning and delivery.

Specialized Machines

Linear Accelerator.—Most radiation treatments to the spine in the United States are delivered by using high-energy photons, which are generated in a linear accelerator from electrons (Fig 9). Electrons are accelerated and bent by a magnet to strike a target made from a high-atomic-number material such as tungsten (Fig 10). On collision with the target, the electrons are rapidly deaccelerated, resulting in the creation of a high-energy photon beam (Fig 11). As these photons interact with tissue, electrons are liberated and deposit ionizing radiation dose in the body. The ionizing radiation damages the DNA of cells either directly through single- and double-stranded DNA breaks or indirectly through the formation of reactive oxygen species and free radicals. A linear accelerator can be used for delivery of both CEBRT and SABR.

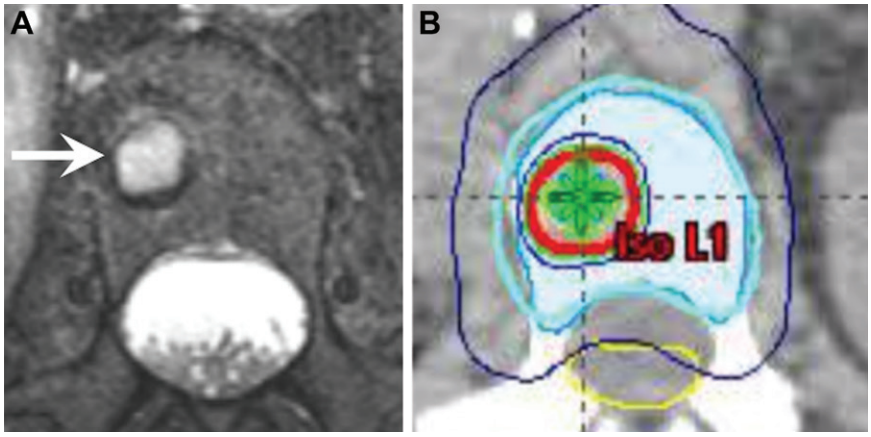

Figure 7. SABR treatment to an L1 metastasis by using simultaneous integrated boost (SIB) technique. **(A)** Preradiation axial T2-weighted MR image shows a metastasis (arrow) in the L1 vertebral body. **(B)** Axial dosimetric CT image obtained for treatment planning shows the red contour line that delineates the prescribed 20-Gy dose to the GTV, and the teal contour line that delineates the prescribed 14-Gy dose to the vertebral body CTV.

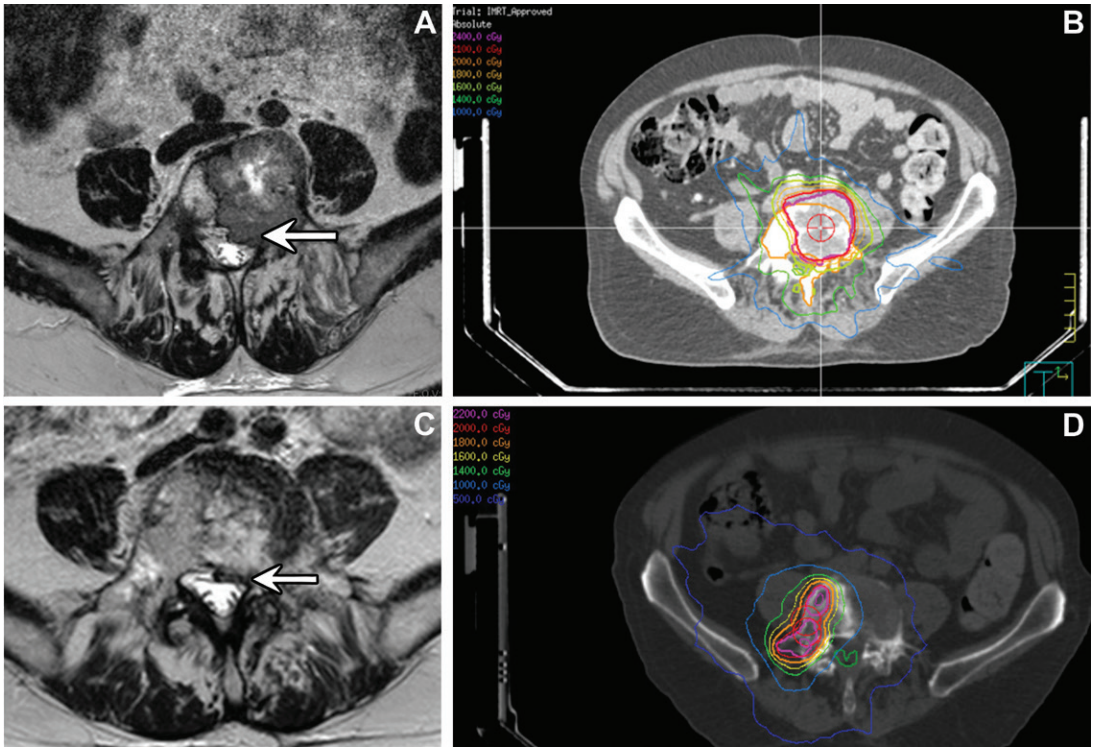

Figure 8. Reirradiation using the SABR simultaneous integrated boost technique in a 60-year-old man with metastatic melanoma to the L5 vertebral body. **(A)** Axial T2-weighted MR image shows an L5 vertebral body metastasis (arrow), with Bilsky grade 2 epidural disease. **(B)** Axial dosimetric CT image shows treatment fields for SABR to L5 with 21 Gy to the GTV (red outline) and 14 Gy to the CTV (green outline). **(C)** Surveillance T2-weighted MR image obtained approximately 5 months after radiation treatment shows residual epidural disease (arrow). **(D)** Axial dosimetric CT image shows salvage radiation with SABR, which was administered with GTV contoured to avoid overlap with the previous high-dose area. The GTV for the reirradiation treatment plan (pink outline) was prescribed to receive 20 Gy in one fraction. Accounting for the previous irradiation, the total dose to the reirradiation GTV was 22 Gy.

CyberKnife.—The CyberKnife (Accuray), developed specifically for stereotactic treatment, is an alternative to the standard linear accelerator for SABR (Fig 12). It consists of a miniature linear accelerator attached to a robotic arm, which allows the use of numerous noncoplanar beams for optimal conformal target coverage with excellent sparing of nearby OARs (Fig 13).

Radiation Therapy Techniques

Three-dimensional Conformal Radiation Therapy.—Historically, radiation was delivered by using two-dimensional (2D) planning based on the anatomic landmarks visualized on radiographs. To ensure appropriate tumor coverage with this approach, large treatment fields were necessary.

Table 4: Dose Constraints for Single-Fraction Irradiation of OARs

OAR	Irradiated Tissue Volume	Maximal Radiation Dose (Gy)	Maximal Radiation Point Dose (Gy)	End Point
Spinal cord	<0.35 cc	10	14	Myelitis
Cauda equina	<5 cc	14	16	Neuritis
Esophagus	<5 cc	20	24	Esophagitis
Lung	<1500 cc (men)	7.2	…	Basic lung function
	<950 cc (women)	7.2	…	Basic lung function
	<37%	8	…	Pneumonitis

Note.—The restricted doses listed are those used for single-fraction irradiation at the authors' institution (The University of Texas Southwestern Medical Center). Maximal point dose is measured as the maximal dose to 0.035 cc.

Table 5: Dose Constraints for Three-Fraction Irradiation of OARs

OAR	Irradiated Tissue Volume	Maximal Radiation Dose (Gy)	Maximal Radiation Point Dose (Gy)	End Point
Spinal cord	<0.35 cc	15.9	22.5	Myelitis
Cauda equina	<5 cc	21.9	25.5	Neuritis
Esophagus	<5 cc	27.9	32.4	Esophagitis
Lung	<1500 cc (men)	20.8	…	Basic lung function
	<950 cc (women)	10.8	…	Basic lung function
	<37%	11.4	…	Pneumonitis

Note.—The restricted doses listed are those used for three-fraction irradiation at the authors' institution (The University of Texas Southwestern Medical Center). The maximal point dose is measured as the maximal dose to 0.035 cc.

Figure 9. Photograph shows the Varian Truebeam (Varian Medical Systems) linear accelerator, which is used for delivery of both CEBRT and SABR.

Since the development of CT, three-dimensional (3D) conformal radiation therapy (CRT) has supplanted 2D planning. By using CT in contouring and treatment planning, 3D CRT has allowed a substantial decrease in the size of the treatment fields required to ensure adequate tumor coverage. Three-dimensional CRT uses fixed beams with multileaf collimators, which are further able to shape the beams, improving the conformality of tumor coverage. Treatment planning uses a forward-planning approach in which the planner must manually place beams into the treatment planning system, with the aim of achieving prescription dose coverage of the target while minimizing the dose to the OARs. This process requires the planner to specify the number of radiation beams, beam energy, beam angles, use of attenuating wedges, and multileaf collimator configuration (Fig 14).

Intensity-modulated Radiation Therapy.—Like 3D CRT, intensity-modulated radiation therapy (IMRT) follows similar basic principles of delivering the prescription radiation doses to the target while limiting doses to OARs. However, in contrast to 3D CRT, IMRT uses both multileaf collimators and dose-rate modification to vary radiation dose intensity across the beam. Additionally, IMRT uses an inverse planning process carried out by sophisticated computer software rather than manual forward planning as in 3D CRT. The modulation of dose intensity results in

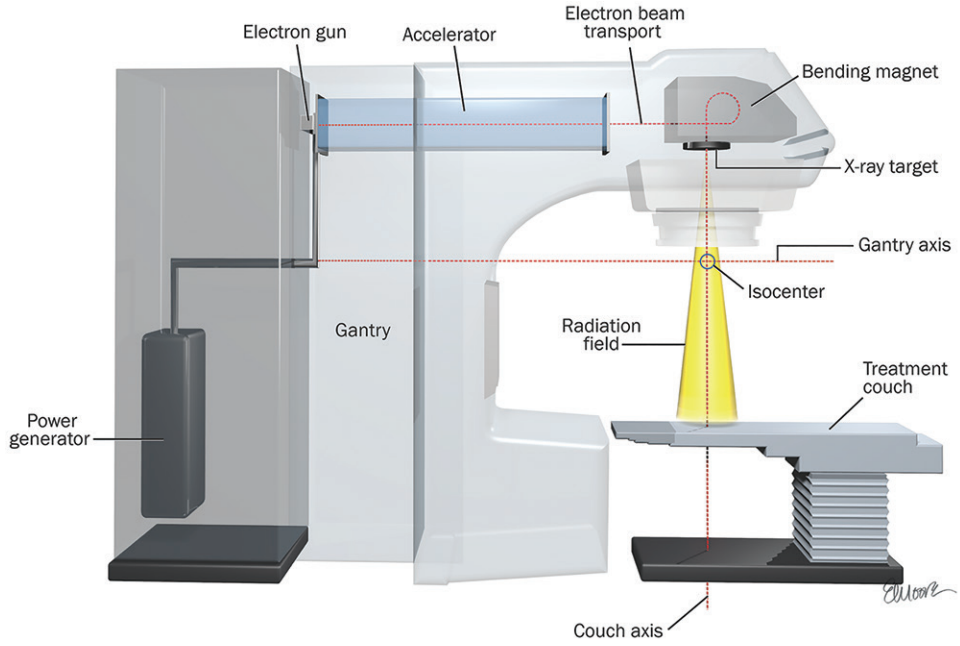

Figure 10. Schematic diagram shows a modern linear accelerator.

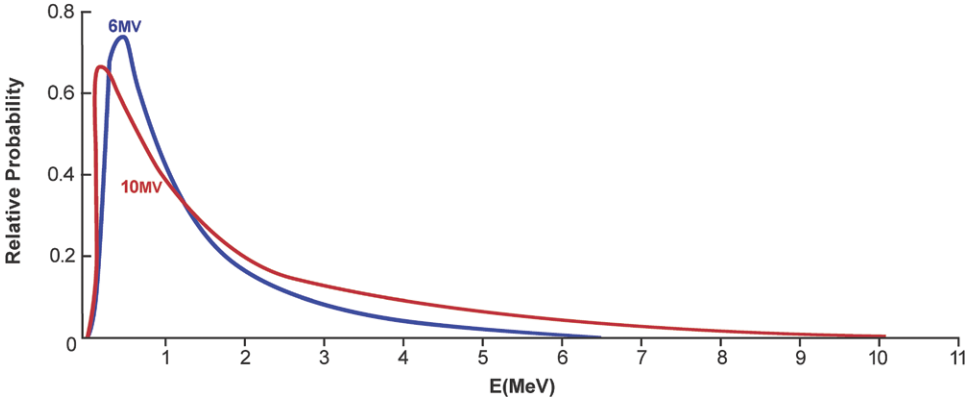

Figure 11. Photon spectra from 6-MV and 10-MV beams. Beams are named on the basis of the maximum potential energy of the electrons as they strike the metal target, but each beam actually consists of a spectrum of particles with different energies. Despite their name, there are relatively few 6-MeV and 10-MeV photons generated from 6-MV and 10-MV beams, respectively.

more conformal treatment plans and improved sparing of nearby OARs. Volumetric modulated arc therapy is a dynamic form of IMRT in which the radiation beam is constantly modulated with continuous radiation delivery as the gantry rotates around the patient (Fig 15).

Charged Particles.—Although photons are the most common particles used in radiation therapy, ionizing radiation can also be produced by heavy charged particles such as protons. While spinal metastases are not currently considered an indication for proton therapy, studies have suggested that protons may provide benefit with reduced spinal cord dose, and further investigation in this area is ongoing (Fig 16) (23,24).

Assessment of Tumor Response at Follow-up Imaging

Standardized criteria for evaluating neoplastic response to therapy at imaging include the widely-used Response Evaluation Criteria in Solid Tumors (RECIST) version 1.1 and the University of Texas MD Anderson Cancer Center (MDACC) criteria. Although version 1.1 of the RECIST criteria does include bone metastases as measurable lesions, the criteria stipulate that osteolytic or mixed osteolytic and osteoblastic lesions can be measured only if soft-tissue extensions of 10 mm or larger can be identified, while osteoblastic lesions are nonmeasurable. However, as spine metastases may involve only bone and may be osteoblastic, the application of this criteria

Figure 12. Photograph shows a CyberKnife treatment system.

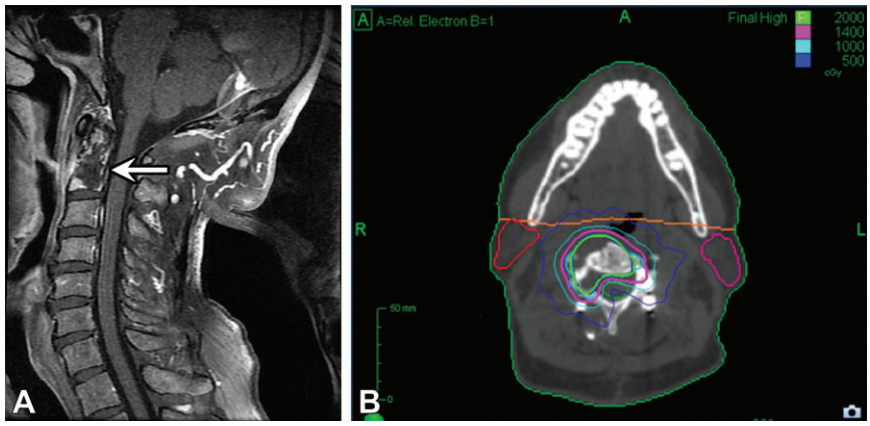

Figure 13. Treatment of metastatic leiomyosarcoma with SABR using the CyberKnife system with the simultaneous integrated boost technique. **(A)** Sagittal T1-weighted MR image shows metastasis of the C2 vertebral body, with a pathologic fracture of the dens (arrow), for which the patient underwent C1–C3 vertebrae posterior fixation and fusion followed by radiation therapy. **(B)** Axial dosimetric CT image obtained for treatment planning. By using our institutional simultaneous integrated boost technique, a total dose of 20 Gy was delivered to the GTV, outlined in bright green, with 14 Gy to the CTV, outlined in fuchsia. Using the CyberKnife system, which allows millimetric precision, negates the need for further expansion to create a PTV volume. Hence, CTV equals PTV, allowing a dose to the spinal cord (dark green outline), to remain well below dosimetric constraints.

to the evaluation of spine metastases in the setting of radiation treatment is limited. MDACC developed criteria with increased specifications for ill-defined and osteolytic lesions of the spine, thus increasing applicability to spine metastases. However, as small changes in epidural and paraspinal disease can significantly alter patient symptomology, true clinical implications may not be captured by these criteria (25–27).

The Spine Response Assessment in Neuro-Oncology (SPINO) Group, a committee of the Response Assessment in Neuro-Oncology Working Group, comprising a panel of experts in spine SABR, has developed recommendations for assessing tumor response at imaging, specifically in the setting of SABR. According to these recommendations, *local control* is defined as the absence of progression within the treated area at serial imaging examinations (2–3 consecutive MRI examinations performed 6–8 weeks apart), and *local progression* is defined as gross increase in tumor volume or linear dimension, any new or progressive tumor within the epidural space, and/or neurologic deterioration attributable to preexisting epidural disease with equivocal change in dimensions of epidural disease at MRI. Pseudoprogression and necrosis must be taken into consideration as these entities can complicate delineation of tumor progression, especially in asymptomatic cases, and may require repeat imaging and biopsy for confirmation (25).

Metallic Artifact Reduction

Subsequent to multilevel spinal stabilization, radiographic visualization of the neural elements is frequently challenging, as visualization of the epidural space can be obscured by susceptibility artifact from metal implants such as the typical

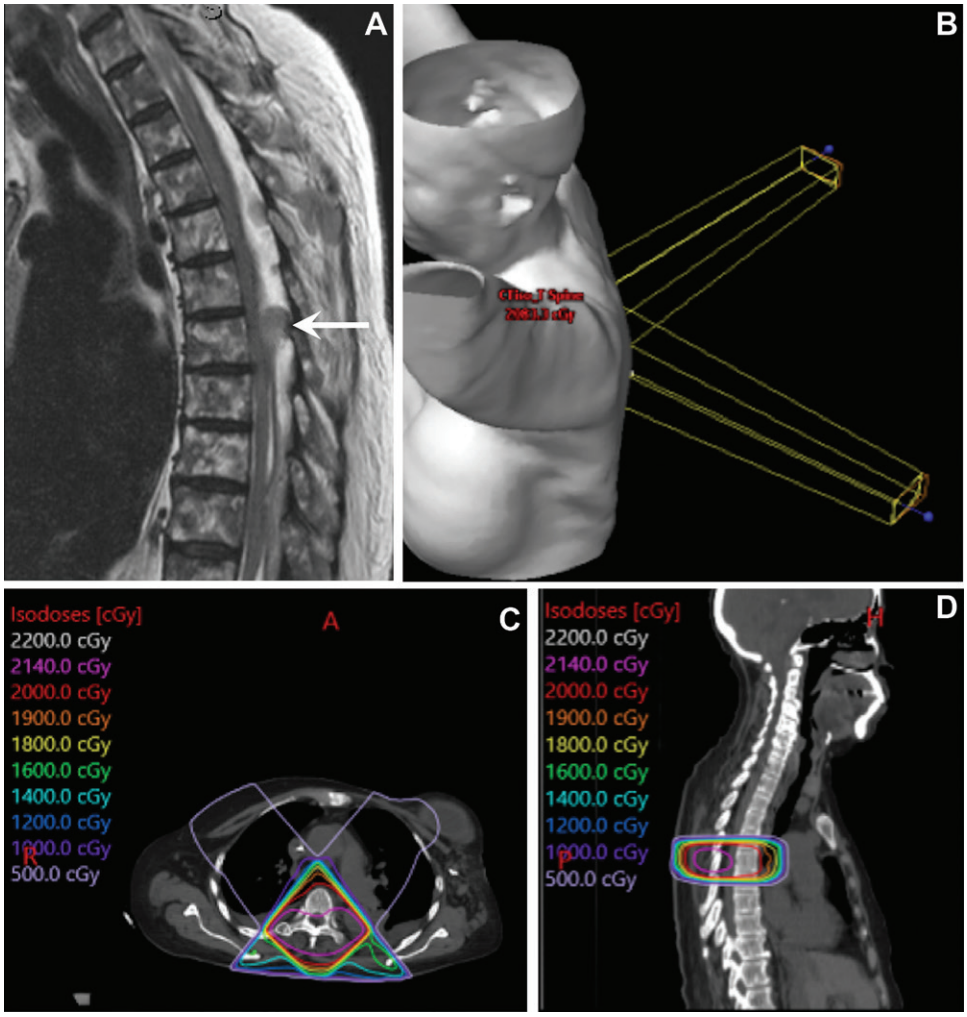

Figure 14. 3D CRT for treatment of metastatic breast cancer. **(A)** Sagittal T2-weighted MR image of the thoracic spine shows numerous osseous metastases, with prominent epidural disease at the T6 vertebral level (arrow). The patient underwent palliative treatment with CEBRT by using 3D CRT. **(B)** 3D volume-rendered CT image obtained for radiation treatment planning shows two oblique fields used for treatment. **(C, D)** Axial **(C)** and sagittal **(D)** dosimetric CT images show the treatment plan.

titanium pedicle screws that are placed adjacent to the area of decompression. Certain scanning techniques can be applied to reduce these artifacts. However, further discussion of these techniques is beyond the scope of this article.

Recently, newer technologies have enabled the design of screws that are non–metal based, such as carbon fiber screws. While technically more challenging to place by surgeons, these screws afford less metal artifact around the site of tumor decompression and can enable better monitoring for tumor recurrence and response to postsurgical oncologic treatment (Fig 17). Furthermore, it is purported that these carbon-based screws can also allow better penetration of radiation to the residual tumor after decompression compared with that of metal screws. However, long-term studies are required to demonstrate whether these technologies improve clinical outcomes.

Dynamic Contrast-enhanced MRI

MRI is critical for detection and follow-up evaluation of primary neoplasms and metastatic disease of the spine. While conventional MRI sequences are helpful in the detection of new metastases, they are limited in the evaluation of response to therapy owing to a lack of specificity in distinguishing viable tumor from posttreatment changes.

One potential solution and an area of active research is dynamic contrast-enhanced MR perfusion imaging. Unlike routine postcontrast imaging, dynamic contrast-enhanced MRI provides temporal information on tumor vascularity and hemodynamics (28) (Fig 18).

Diffusion-weighted Imaging

Diffusion-weighted imaging has been shown to be accurate for initial detection of vertebral metastases. In patients who have shown clinical improvement following radiation therapy for vertebral

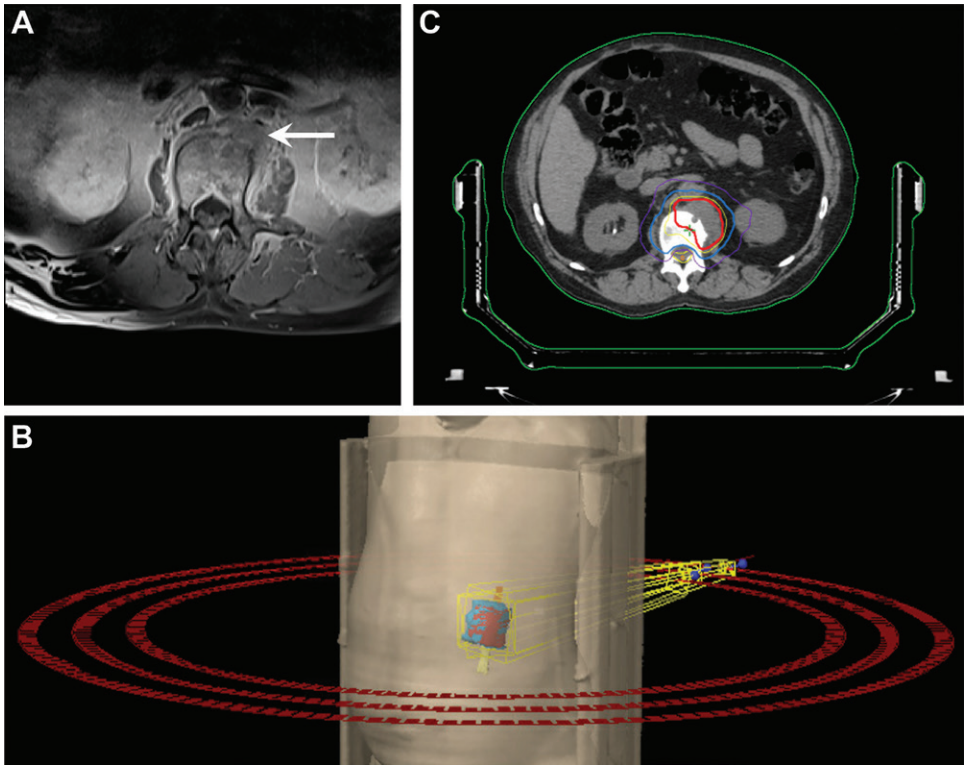

Figure 15. Treatment of metastatic hepatocellular carcinoma with volumetric modulated arc therapy (VMAT). **(A)** Axial T1-weighted MR image shows a metastasis involving L1-L2 vertebrae (arrow). **(B, C)** Volume-rendered 3D CT image **(B)** shows SABR with VMAT, and the axial dosimetric CT image **(C)** shows the simultaneous integrated boost technique, with a total of 20 Gy to the GTV (red outline) and 14 Gy to the PTV (blue outline).

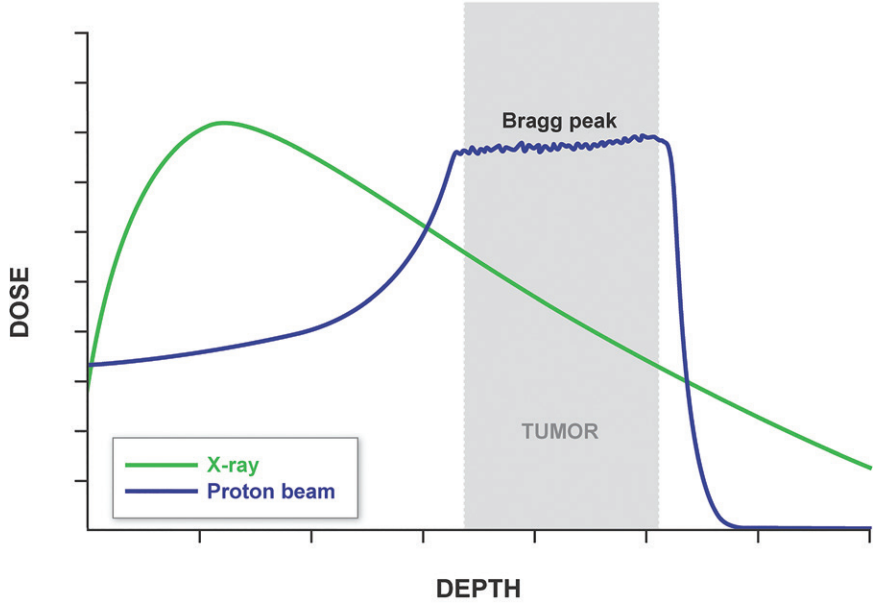

Figure 16. Graph shows the relative dose and depth characteristics of photon and proton beams. The use of protons, which are generated from hydrogen gas and accelerated in a cyclotron or synchrotron, has become increasingly common over the past few decades for treatment of pediatric central nervous system tumors. There is interest in expanding proton use to other disease sites as well, with mixed consensus on whether charged particles provide a benefit over irradiation with photons. Unlike photons, protons have the advantage of the Bragg peak, which results in extremely steep radiation dose fall-off and spares normal tissue located deep relative to the target. However, treatment with protons also has the disadvantage of requiring an additional margin to account for uncertainty related to the exact point at which radiation dose fall-off occurs.

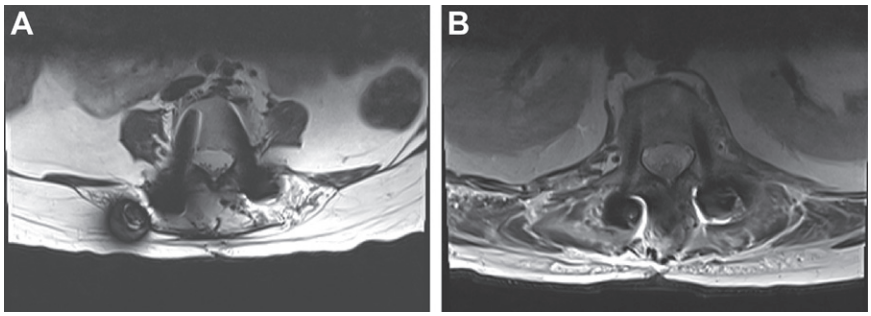

Figure 17. Reduced artifact associated with carbon fiber screws for spinal fixation. **(A)** Axial T2-weighted MR image shows susceptibility artifact related to titanium spinal fixation hardware, with suboptimal visualization of portions of the spinal canal. **(B)** Axial T2-weighted MR image shows reduced artifact associated with carbon fiber screws used for spinal fixation and thus improved visualization of the epidural space.

metastases, an increase in apparent diffusion coefficient values has been demonstrated in metastatic lesions in several studies (29).

Treatment Effects

Radiation therapy has increasingly become an excellent option for treatment of vertebral metastases. Ablative doses administered with newer stereotactic techniques can achieve higher rates of tumor control and improvement in pain but still carry the risk of adverse effects. Thus, it is imperative to be aware of treatment-related effects, some of which may manifest at imaging.

Pain Flare

Pain flare, an acute worsening of pain, is a common toxic effect associated with spine irradiation. Reported incidence of pain flare with SABR ranges from 25% to almost 70%, and it typically occurs during or soon after radiation treatment (30,31). The suspected cause is edema secondary to treatment-related inflammation. Hence, management consists of pain control with analgesic medication and a short course of steroid therapy to reduce inflammation and edema; prophylactic administration of steroid therapy is also an option (32).

Esophagitis

Esophagitis is an acute toxic effect associated with radiation therapy for spinal metastases located in the lower cervical and thoracic spine. However, with the evolution of radiation therapy techniques and increased use of IMRT for metastases located in close proximity to the esophagus, incidence of severe esophageal toxic effects has decreased dramatically (33). Various institutional series have demonstrated dose-dependent grade 3 or higher esophageal toxic effects rates of approximately 6% of patients following SABR, with all cases occurring in patients receiving systemic therapy shortly before or after radiation therapy (34–36). Avoiding systemic therapy close to the time of radiation therapy, limiting the volumetric dose to 2.5 cc of the esophagus to less than 14 Gy, and avoiding postradiation esophageal procedures is recommended to limit esophageal toxic effects (35).

Dermatitis

Low-grade hyperpigmentation or dermatitis has been reported in both the acute and late settings following single-fraction SABR for spine metastases, with acute and late incidences of approximately 17% and 22%, respectively (14). There is no increased risk in the incidence or severity of dermatitis following an initial course of reirradiation (37). However, multiple courses of reirradiation to the same area have demonstrated a risk of grade 3 or higher dermatitis (38).

Radiation-induced Bone Marrow Changes

Radiation-induced bone marrow changes can be detected at MRI as early as 2 weeks following initiation of radiation therapy. At short-τ inversion-recovery (STIR) imaging, these early changes may appear with high signal intensity, reflecting early marrow edema. Approximately 3–6 weeks following initiation of radiation therapy, normal marrow elements are replaced by fat, resulting in heterogeneous signal intensity of the affected vertebrae. Late changes, occurring 6 weeks to 14 months following radiation therapy, manifest as either homogeneous fatty replacement of the irradiated vertebral segments or as regions of peripheral intermediate signal intensity, representing regeneration of hematopoietic tissue, with central marrow fat (39).

Osseous Pseudoprogression

Pseudoprogression is defined as a treatment-related transient tumor growth mimicking true progression. This is more commonly described in the brain and other anatomic sites but recently

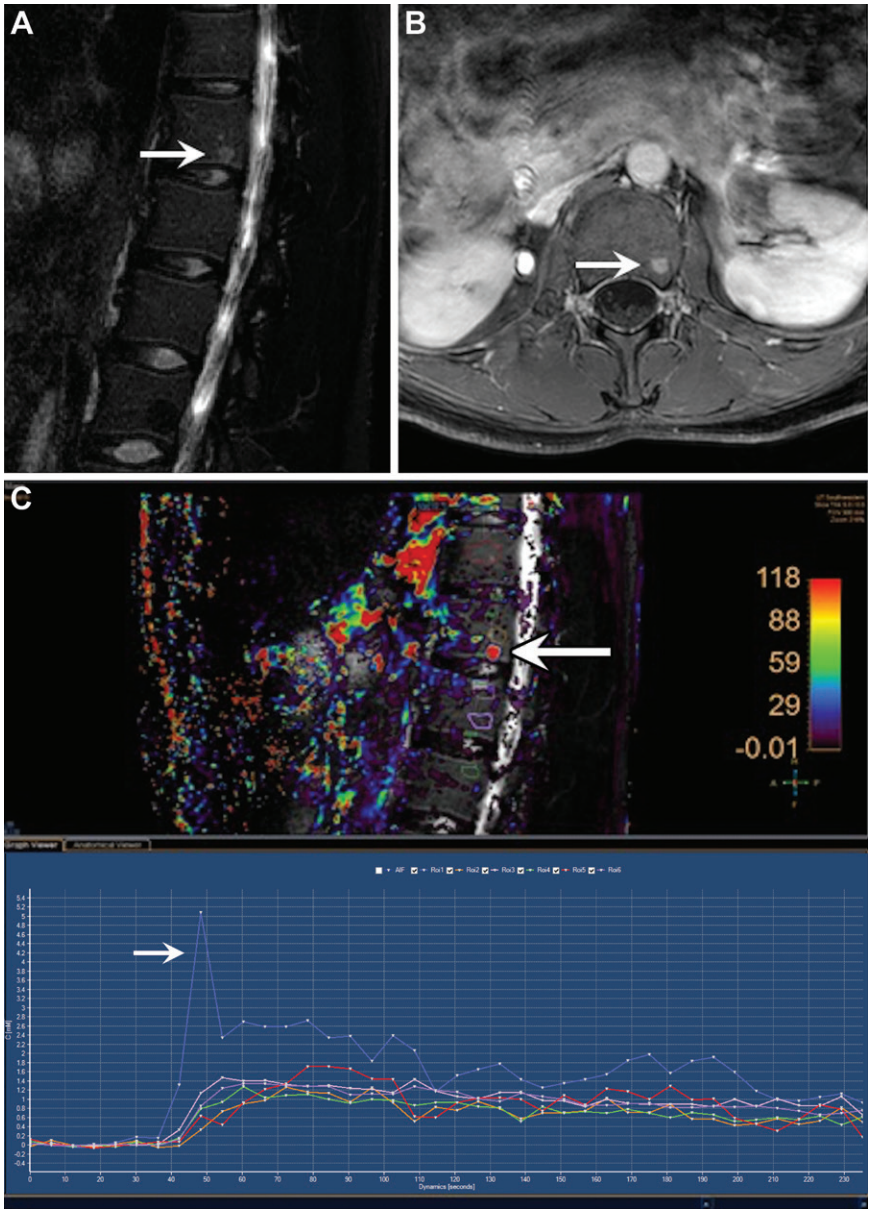

Figure 18. Dynamic contrast-enhanced perfusion MRI for characterization of an indeterminate spine lesion in a 32-year-old woman with malignant hemangiopericytoma who underwent spine MRI for surveillance. **(A, B)** Sagittal STIR **(A)** and axial contrast-enhanced T1-weighted **(B)** MR images of the spine show a 7-mm lesion (arrow) in the T1 vertebral body. **(C)** Dynamic contrast-enhanced perfusion MR image with kinetic analysis shows that the lesion in question (arrows, blue kinetic curve) demonstrates a pattern of rapid wash-in and fast initial washout, supporting the clinical suspicion for metastatic disease.

has also been described in the spine. As in other sites, imaging shows growth of treated lesions in the 3–6 months following radiation therapy, with a decrease in size of the lesions at 6–12-month posttreatment imaging, not attributable to chemotherapy (40).

Vertebral Compression Fracture

Vertebral compression fracture (VCF) is one of the most common toxic effects associated with spinal irradiation, with prevalence rates in the literature ranging from 10% to 40% for patients receiving SABR to the spine (10,41,42). This is thought to be due to radiation-induced late effects within the tumor and bone tissue that weaken the vertebral body (43).

Risk factors for VCF include older age, spinal misalignment or deformity, higher dose per fraction, baseline VCF, lytic tumors, and more than 40%–50% tumor involvement of the vertebral body (44). Treatment with doses greater than 20 Gy per fraction has been found to predict for VCF (45). Additionally, patients with a solitary spinal metastasis may be at increased risk of new or progressive VCF following SBRT owing to a tendency for more aggressive treatment with higher doses. Performing pre-SBRT MRI for delineation of treatment targets leads to increased target volume accuracy and a lower volume of vertebral body irradiated, which has been found to be protective against development of VCF (46).

Percutaneous vertebral augmentation can be considered to improve patient pain and morbidity following radiation-induced VCF (47) (Fig 19). Given the significant risk of VCF in the setting of radiation therapy to the spine, prophylactic

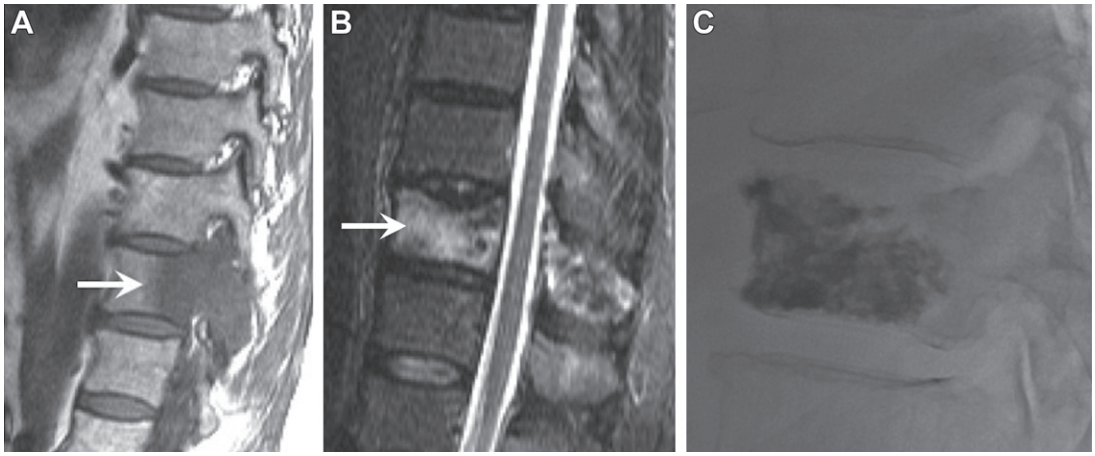

Figure 19. Vertebral compression fracture in an 81-year-old man with prostate cancer with spinal metastases who presented with low back pain following radiation therapy. **(A)** Sagittal T1-weighted MR image shows infiltrative metastatic disease involving the T11 vertebral body and posterior elements (arrow), which was treated with radiation therapy. The patient subsequently developed worsening low back pain. **(B)** Postradiation therapy sagittal STIR MR image of the spine shows evidence of prior T11 metastasis treatment with new bone marrow edema and deformity of the superior endplate (arrow), indicative of an acute vertebral compression fracture. **(C)** Sagittal fluoroscopic image was obtained during percutaneous vertebroplasty, after which the patient reported improvement in pain symptoms.

vertebroplasty performed within 1 month following SABR has been shown to be a promising measure to provide long-term pain control (48).

Radiation Myelopathy

Radiation myelopathy is a rare delayed complication associated with high cumulative doses to the spinal cord (49). In patients undergoing single-fraction treatment, a maximum point dose of 14 Gy to the spinal cord is associated with a less than 1% risk of myelopathy (22). Myelopathy can be classified as a transient early-delayed reaction or late-delayed reaction (50).

Early-delayed injury, also known as L'hermitte syndrome, is self-limited, typically occurs after a latent period of 2–4 months after treatment, and is characterized by transient shocklike paresthesias or numbness radiating from the neck to the extremities on neck flexion. This is followed by complete clinical recovery over the following 3–6 months and does not result in permanent myelopathy. This is attributed to a transient demyelination owing to radiation-induced oligodendroglial cell injury (50,51).

Late-delayed injury is irreversible and is typically not seen earlier than 6 months after completion of treatment (51). Although the occurrence of late injury is exceedingly rare in the era of 3D conformal conventionally fractionated radiation therapy, this has reemerged secondary to increasing SBRT practice, where the high doses of radiation coupled with small intrafraction motion of 1–2 mm can increase spinal cord radiation dose (52,53). Signs and symptoms, which may range from minor motor and sensory deficits to Brown-Séquard syndrome, typically progress over several months, although acute onset of symptoms over hours to days is possible. Late-delayed injury is thought to be due to a combination of radiation-induced oligodendroglial injury and microvascular injury (50,51).

Radiation-induced myelopathy is a diagnosis of exclusion, and the following must be considered for its diagnosis: *(a)* radiation therapy to the cord in doses sufficient to cause injury, *(b)* neurologic signs and symptoms corresponding to the irradiated cord segment, *(c)* symptoms occurring after a latent period of at least 6 months, and *(d)* lack of cord metastases or primary lesions. Characteristic MRI findings of radiation myelopathy include T1-weighted hypointensity and T2-weighted hyperintensity of the involved cord, with or without enhancement (51) (Fig 20).

Differentiation of radiation myelopathy from primary spinal cord tumors or metastases may be challenging given the overlapping imaging findings. Fluorine-18 (^{18}F) fluorodeoxyglucose (FDG) PET/CT may be beneficial, as radiation-induced changes within the cord should not show pathologic ^{18}F-FDG uptake, whereas pathologic uptake would be seen in the case of cord malignancy (54) (Fig 21).

Limiting radiation dose, adopting a strict technical protocol with patient immobilization, and using intrafraction 3D image guidance have helped mitigate the risk of radiation myelopathy (52,53).

Radiation Myositis

Myositis is a rare delayed complication of high-dose radiation therapy, with a prevalence estimated at 1.9%. Most cases occur following single-fraction

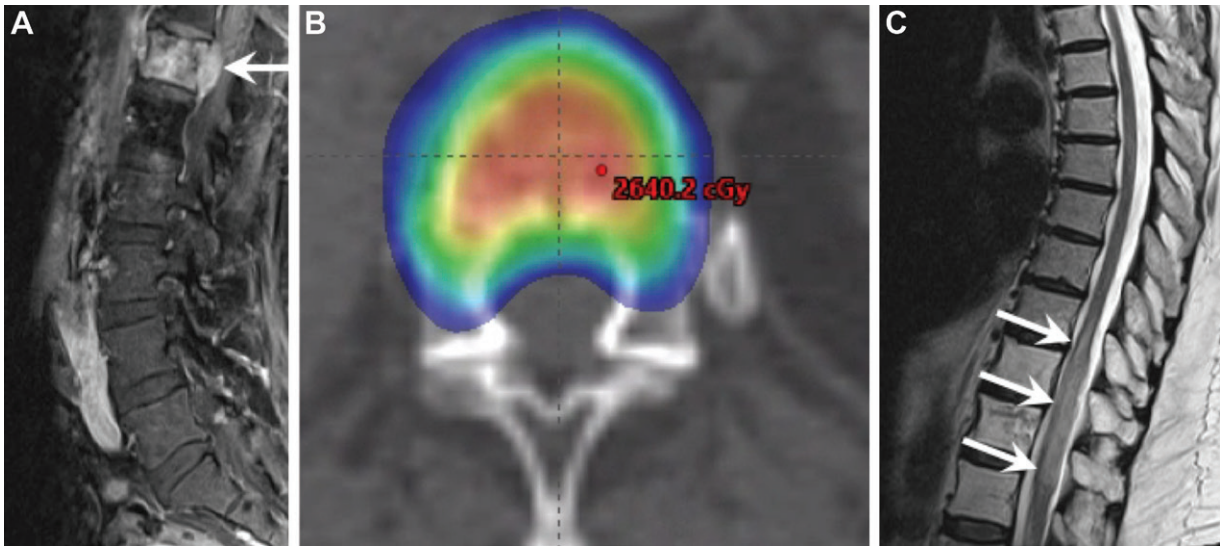

Figure 20. Radiation myelopathy in a 68-year-old woman with metastatic renal cell carcinoma to the spine who underwent radiation therapy. **(A)** Sagittal contrast-enhanced T1-weighted MR image of the spine shows infiltrative metastatic disease involving the T12 vertebral body with extraosseous soft-tissue extension into the ventral epidural space (arrow) for which she underwent radiation therapy. **(B)** Axial dosimetric CT image shows the radiation treatment plan. She subsequently developed paraplegia 26 months following completion of radiation therapy. **(C)** Postradiation therapy sagittal T2-weighted MR image of the spine shows abnormal T2 signal intensity within the spinal cord at the treated level (arrows), reflective of radiation myelopathy, which was managed supportively with high-dose steroid therapy, bevacizumab, and hyperbaric oxygen, with eventual partial improvement in lower extremity strength.

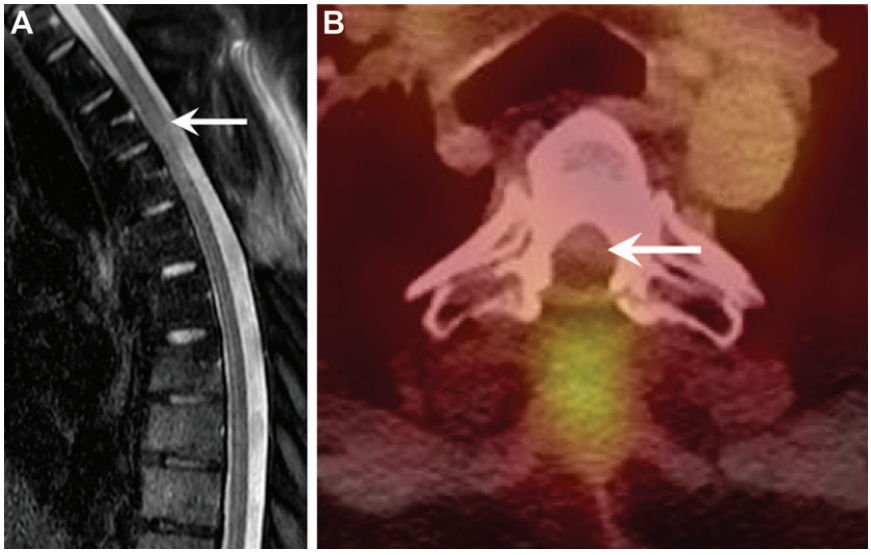

Figure 21. Radiation myelopathy in a 45-year-old woman who underwent thoracic laminectomies and radiation therapy for a T3 vertebral plasmacytoma. **(A)** Sagittal STIR MR image obtained 7 months after completion of radiation therapy shows abnormal signal intensity (arrow) within the spinal cord, thought to be due to radiation myelopathy. **(B)** Axial fused ^{18}F-FDG PET/CT image obtained concurrently for staging shows absence of ^{18}F-FDG uptake (arrow) within the spinal cord, confirming the suspected diagnosis of radiation myelopathy. Low-level tracer uptake in the surgical bed was thought to be due to expected postsurgical change.

SABR to the lumbar spine, with patients typically presenting with back pain before the development of imaging changes. The median reported time of imaging evidence of myositis is 4–5 months following completion of radiation therapy, with the affected muscles correlating with the treatment ports. At imaging, radiation-induced myositis appears as T2-weighted hyperintensity, reflecting edema, with associated patchy enhancement of the affected muscles. Necrosis may also be present (Fig 22). Recognition of myositis is important to differentiate myositis from residual or recurrent tumor owing to overlapping imaging findings with these entities. Management consists of analgesic agents and steroid therapy for pain control and reduction of inflammation, respectively (55).

Conclusion

Radiation therapy is an important treatment modality for vertebral metastases, with impressive rates of palliative benefit as well as local control. Historically, partnership between radiation oncologists and radiologists has been limited by different work flows, physical locations, and computer systems. However, collaboration between radiologists and radiation oncologists is vital, as accurate assessment of pretreatment imaging is essential to guide multidisciplinary management and determine the

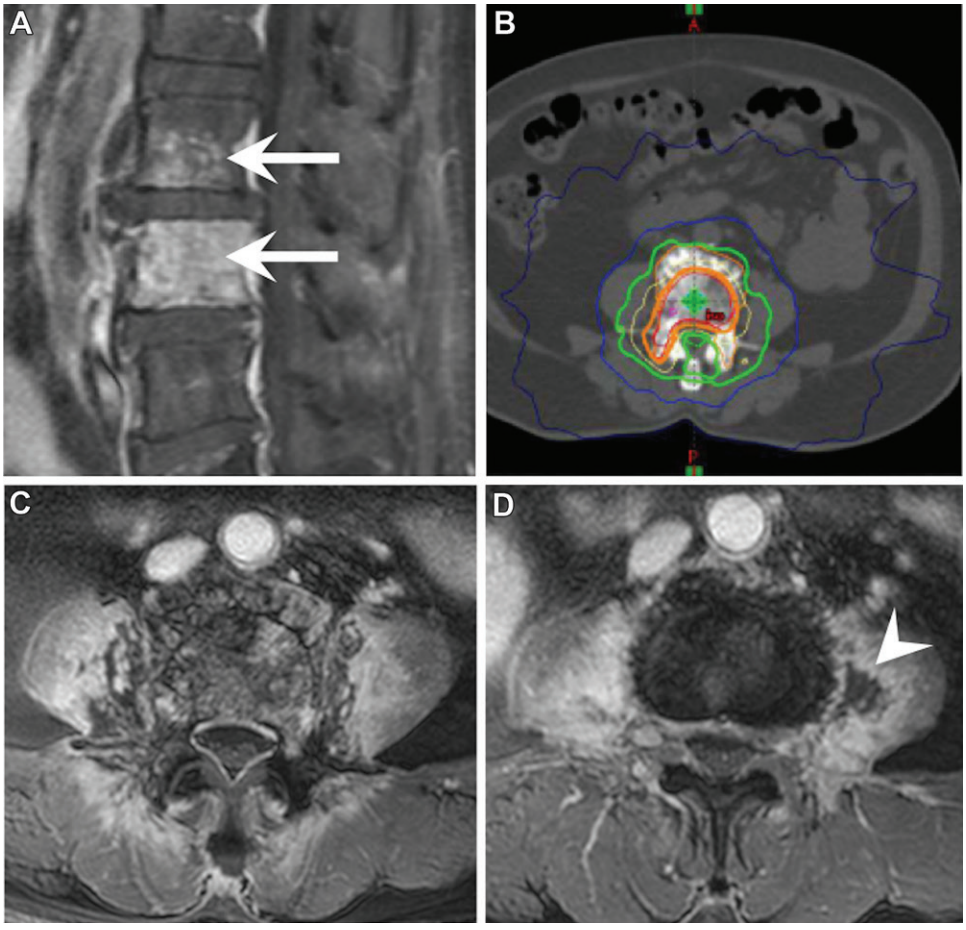

Figure 22. Radiation-induced myositis in a 71-year-old woman with a history of lobular carcinoma of the right breast. The patient underwent MRI of the spine for back pain and right L4 radiculopathy not controlled by medications. **(A)** Sagittal contrast-enhanced T1-weighted image shows metastatic disease involving the L3 and L4 vertebral bodies (arrows), which were treated with radiation therapy. **(B)** Axial dosimetric CT image shows radiation planning. The patient underwent treatment with SABR, with a total dose of 20 Gy to the GTV and 14 Gy to the CTV to the L3 and L4 vertebral bodies. **(C, D)** Surveillance axial contrast-enhanced T1-weighted MR images obtained 3 months after radiation therapy show interval development of enhancement in the medial psoas muscles bilaterally, reflective of myositis. Necrosis is depicted as patchy areas of nonenhancement (arrowhead in **D**).

optimal treatment plan for each patient. Familiarity with radiation treatment planning and posttreatment complications associated with spinal irradiation is also crucial for radiologists in the interpretation of posttreatment images and detection of treatment-related toxic effects.

***Disclosures of Conflicts of Interest.*—F.F.U.** *Activities related to the present article:* disclosed no relevant relationships. *Activities not related to the present article:* institutional grant from the Texas Alzheimer's research and care consortium. *Other activities:* disclosed no relevant relationships. **A.A.** *Activities related to the present article:* disclosed no relevant relationships. *Activities not related to the present article:* institutional support for Authentic 4D consultancy (second opinion/reads); expert testimony as an expert witness. *Other activities:* disclosed no relevant relationships.

References

1. Ciftdemir M, Kaya M, Selcuk E, Yalniz E. Tumors of the spine. World J Orthop 2016;7(2):109–116.
2. Gerszten PC. Spine metastases: from radiotherapy, surgery, to radiosurgery. Neurosurgery 2014;61(suppl 1):16–25.
3. Laufer I, Rubin DG, Lis E, et al. The NOMS framework: approach to the treatment of spinal metastatic tumors. Oncologist 2013;18(6):744–751.
4. Bilsky MH, Laufer I, Fourney DR, et al. Reliability analysis of the epidural spinal cord compression scale. J Neurosurg Spine 2010;13(3):324–328.
5. Patchell RA, Tibbs PA, Regine WF, et al. Direct decompressive surgical resection in the treatment of spinal cord compression caused by metastatic cancer: a randomised trial. Lancet 2005;366(9486):643–648.
6. Fisher CG, DiPaola CP, Ryken TC, et al. A novel classification system for spinal instability in neoplastic disease: an evidence-based approach and expert consensus from the Spine Oncology Study Group. Spine 2010;35(22):E1221–E1229.
7. Fourney DR, Frangou EM, Ryken TC, et al. Spinal instability neoplastic score: an analysis of reliability and validity from the spine oncology study group. J Clin Oncol 2011;29(22):3072–3077.
8. Rock JP, Ryu S, Shukairy MS, et al. Postoperative radiosurgery for malignant spinal tumors. Neurosurgery 2006;58(5):891–898; discussion 891–898.
9. Moulding HD, Elder JB, Lis E, et al. Local disease control after decompressive surgery and adjuvant high-dose single-fraction radiosurgery for spine metastases. J Neurosurg Spine 2010;13(1):87–93.

10. Glicksman RM, Tjong MC, Neves-Junior WFP, et al. Stereotactic Ablative Radiotherapy for the Management of Spinal Metastases: A Review. JAMA Oncol 2020;6(4):567–577.
11. Sahgal A, Bilsky M, Chang EL, et al. Stereotactic body radiotherapy for spinal metastases: current status, with a focus on its application in the postoperative patient. J Neurosurg Spine 2011;14(2):151–166.
12. Maranzano E, Bellavita R, Rossi R, et al. Short-course versus split-course radiotherapy in metastatic spinal cord compression: results of a phase III, randomized, multicenter trial. J Clin Oncol 2005;23(15):3358–3365.
13. Yamada Y, Bilsky MH, Lovelock DM, et al. High-dose, single-fraction image-guided intensity-modulated radiotherapy for metastatic spinal lesions. Int J Radiat Oncol Biol Phys 2008;71(2):484–490.
14. Moussazadeh N, Lis E, Katsoulakis E, et al. Five-Year Outcomes of High-Dose Single-Fraction Spinal Stereotactic Radiosurgery. Int J Radiat Oncol Biol Phys 2015;93(2):361–367.
15. Howell DD, James JL, Hartsell WF, et al. Single-fraction radiotherapy versus multifraction radiotherapy for palliation of painful vertebral bone metastases-equivalent efficacy, less toxicity, more convenient: a subset analysis of Radiation Therapy Oncology Group trial 97-14. Cancer 2013;119(4):888–896.
16. Rades D, Huttenlocher S, Šegedin B, et al. Single-Fraction Versus 5-Fraction Radiation Therapy for Metastatic Epidural Spinal Cord Compression in Patients With Limited Survival Prognoses: Results of a Matched-Pair Analysis. Int J Radiat Oncol Biol Phys 2015;93(2):368–372.
17. Rades D, Šegedin B, Conde-Moreno AJ, et al. Radiotherapy With 4 Gy × 5 Versus 3 Gy × 10 for Metastatic Epidural Spinal Cord Compression: Final Results of the SCORE-2 Trial (ARO 2009/01). J Clin Oncol 2016;34(6):597–602.
18. Cox BW, Spratt DE, Lovelock M, et al. International Spine Radiosurgery Consortium consensus guidelines for target volume definition in spinal stereotactic radiosurgery. Int J Radiat Oncol Biol Phys 2012;83(5):e597–e605.
19. Guckenberger M, Sweeney RA, Flickinger JC, et al. Clinical practice of image-guided spine radiosurgery: results from an international research consortium. Radiat Oncol 2011;6(1):172.
20. Guckenberger M, Hawkins M, Flentje M, Sweeney RA. Fractionated radiosurgery for painful spinal metastases: DOSIS—a phase II trial. BMC Cancer 2012;12(1):530.
21. Tseng C-L, Soliman H, Myrehaug S, et al. Imaging-Based Outcomes for 24 Gy in 2 Daily Fractions for Patients with de Novo Spinal Metastases Treated With Spine Stereotactic Body Radiation Therapy (SBRT). Int J Radiat Oncol Biol Phys 2018;102(3):499–507.
22. Katsoulakis E, Jackson A, Cox B, Lovelock M, Yamada Y. A Detailed Dosimetric Analysis of Spinal Cord Tolerance in High-Dose Spine Radiosurgery. Int J Radiat Oncol Biol Phys 2017;99(3):598–607.
23. Paganetti H. Range uncertainties in proton therapy and the role of Monte Carlo simulations. Phys Med Biol 2012;57(11):R99–R117.
24. Rief H, Chaudhri N, Tonndorf-Martini E, et al. Intensity-modulated radiotherapy versus proton radiotherapy versus carbon ion radiotherapy for spinal bone metastases: a treatment planning study. J Appl Clin Med Phys 2015;16(6):186–194.
25. Thibault I, Chang EL, Sheehan J, et al. Response assessment after stereotactic body radiotherapy for spinal metastasis: a report from the SPIne response assessment in Neuro-Oncology (SPINO) group. Lancet Oncol 2015;16(16):e595–e603.
26. Therasse P, Arbuck SG, Eisenhauer EA, et al. New guidelines to evaluate the response to treatment in solid tumors. European Organization for Research and Treatment of Cancer, National Cancer Institute of the United States, National Cancer Institute of Canada. J Natl Cancer Inst 2000;92(3):205–216.
27. Costelloe CM, Chuang HH, Madewell JE, Ueno NT. Cancer Response Criteria and Bone Metastases: RECIST 1.1, MDA and PERCIST. J Cancer 2010;1:80–92.
28. Chu S, Karimi S, Peck KK, et al. Measurement of blood perfusion in spinal metastases with dynamic contrast-enhanced magnetic resonance imaging: evaluation of tumor response to radiation therapy. Spine 2013;38(22):E1418–E1424.
29. Herneth AM, Philipp MO, Naude J, et al. Vertebral metastases: assessment with apparent diffusion coefficient. Radiology 2002;225(3):889–894.
30. Chiang A, Zeng L, Zhang L, et al. Pain flare is a common adverse event in steroid-naïve patients after spine stereotactic body radiation therapy: a prospective clinical trial. Int J Radiat Oncol Biol Phys 2013;86(4):638–642.
31. Pan HY, Allen PK, Wang XS, et al. Incidence and predictive factors of pain flare after spine stereotactic body radiation therapy: secondary analysis of phase 1/2 trials. Int J Radiat Oncol Biol Phys 2014;90(4):870–876.
32. McDonald R, Chow E, Rowbottom L, DeAngelis C, Soliman H. Incidence of pain flare in radiation treatment of bone metastases: A literature review. J Bone Oncol 2014;3(3-4):84–89.
33. Sprave T, Verma V, Förster R, et al. Radiation-induced acute toxicities after image-guided intensity-modulated radiotherapy versus three-dimensional conformal radiotherapy for patients with spinal metastases (IRON-1 trial) : First results of a randomized controlled trial. Strahlenther Onkol 2018;194(10):911–920.
34. Abelson JA, Murphy JD, Loo BW Jr, et al. Esophageal tolerance to high-dose stereotactic ablative radiotherapy. Dis Esophagus 2012;25(7):623–629.
35. Cox BW, Jackson A, Hunt M, Bilsky M, Yamada Y. Esophageal toxicity from high-dose, single-fraction paraspinal stereotactic radiosurgery. Int J Radiat Oncol Biol Phys 2012;83(5):e661–e667.
36. Stephans KL, Djemil T, Diaconu C, et al. Esophageal dose tolerance to hypofractionated stereotactic body radiation therapy: risk factors for late toxicity. Int J Radiat Oncol Biol Phys 2014;90(1):197–202.
37. Kawashiro S, Harada H, Katagiri H, et al. Reirradiation of spinal metastases with intensity-modulated radiation therapy: an analysis of 23 patients. J Radiat Res (Tokyo) 2016;57(2):150–156.
38. Katsoulakis E, Riaz N, Cox B, et al. Delivering a third course of radiation to spine metastases using image-guided, intensity-modulated radiation therapy. J Neurosurg Spine 2013;18(1):63–68.
39. Stevens SK, Moore SG, Kaplan ID. Early and late bone-marrow changes after irradiation: MR evaluation. AJR Am J Roentgenol 1990;154(4):745–750.
40. Amini B, Beaman CB, Madewell JE, et al. Osseous Pseudoprogression in Vertebral Bodies Treated with Stereotactic Radiosurgery: A Secondary Analysis of Prospective Phase I/II Clinical Trials. AJNR Am J Neuroradiol 2016;37(2):387–392.
41. Boehling NS, Grosshans DR, Allen PK, et al. Vertebral compression fracture risk after stereotactic body radiotherapy for spinal metastases. J Neurosurg Spine 2012;16(4):379–386.
42. Chang JH, Gandhidasan S, Finnigan R, et al. Stereotactic Ablative Body Radiotherapy for the Treatment of Spinal Oligometastases. Clin Oncol (R Coll Radiol) 2017;29(7):e119–e125.
43. Al-Omair A, Smith R, Kiehl T-R, et al. Radiation-induced vertebral compression fracture following spine stereotactic radiosurgery: clinicopathological correlation. J Neurosurg Spine 2013;18(5):430–435.
44. Faruqi S, Tseng C-L, Whyne C, et al. Vertebral Compression Fracture After Spine Stereotactic Body Radiation Therapy: A Review of the Pathophysiology and Risk Factors. Neurosurgery 2018;83(3):314–322.
45. Sahgal A, Atenafu EG, Chao S, et al. Vertebral compression fracture after spine stereotactic body radiotherapy: a multi-institutional analysis with a focus on radiation dose and the spinal instability neoplastic score. J Clin Oncol 2013;31(27):3426–3431.
46. Jawad MS, Fahim DK, Gerszten PC, et al. Vertebral compression fractures after stereotactic body radiation therapy: a large, multi-institutional, multinational evaluation. J Neurosurg Spine 2016;24(6):928–936.

47. Kassamali RH, Ganeshan A, Hoey ETD, Crowe PM, Douis H, Henderson J. Pain management in spinal metastases: the role of percutaneous vertebral augmentation. Ann Oncol 2011;22(4):782–786.
48. Wardak Z, Bland R, Ahn C, et al. A Phase 2 Clinical Trial of SABR Followed by Immediate Vertebroplasty for Spine Metastases. Int J Radiat Oncol Biol Phys 2019;104(1):83–89.
49. Hall WA, Stapleford LJ, Hadjipanayis CG, Curran WJ, Crocker I, Shu H-KG. Stereotactic body radiosurgery for spinal metastatic disease: an evidence-based review. Int J Surg Oncol 2011;2011:979214.
50. Wong CS, Fehlings MG, Sahgal A. Pathobiology of radiation myelopathy and strategies to mitigate injury. Spinal Cord 2015;53(8):574–580.
51. Science Direct. Radiation Myelopathy: an overview. https://www.sciencedirect.com/topics/medicine-and-dentistry/radiation-myelopathy. Accessed March 6, 2021.
52. Sahgal A, Weinberg V, Ma L, et al. Probabilities of radiation myelopathy specific to stereotactic body radiation therapy to guide safe practice. Int J Radiat Oncol Biol Phys 2013;85(2):341–347.
53. Chang JH, Shin JH, Yamada YJ, et al. Stereotactic Body Radiotherapy for Spinal Metastases: What are the Risks and How Do We Minimize Them? Spine 2016;41(suppl 20):S238–S245.
54. Kadir T, Sarica FB, Ozgur K, Cekinmez M, Nur AM. Delayed radiation myelopathy: Differential diagnosis with positron emission tomography/computed tomography examination. Asian J Neurosurg 2012;7(4):206–209.
55. Lockney DT, Jia AY, Lis E, et al. Myositis following spine radiosurgery for metastatic disease: a case series. J Neurosurg Spine 2018;28(4):416–421.